LBL-11777
Preprint

Lawrence Berkeley Laboratory
UNIVERSITY OF CALIFORNIA

Materials & Molecular Research Division

RECEIVED
LAWRENCE
BERKELEY LABORATORY
MAY 7 1982
LIBRARY AND
DOCUMENTS SECTION

Submitted to the Welding Journal

WELDABILITY OF GRAIN-REFINED Fe-12Ni-0.25Ti STEEL FOR CRYOGENIC APPLICATIONS

D.E. Williams and J.W. Morris, Jr.

June 1981

TWO-WEEK LOAN COPY

This is a Library Circulating Copy which may be borrowed for two weeks. For a personal retention copy, call Tech. Info. Division, Ext. 6782.

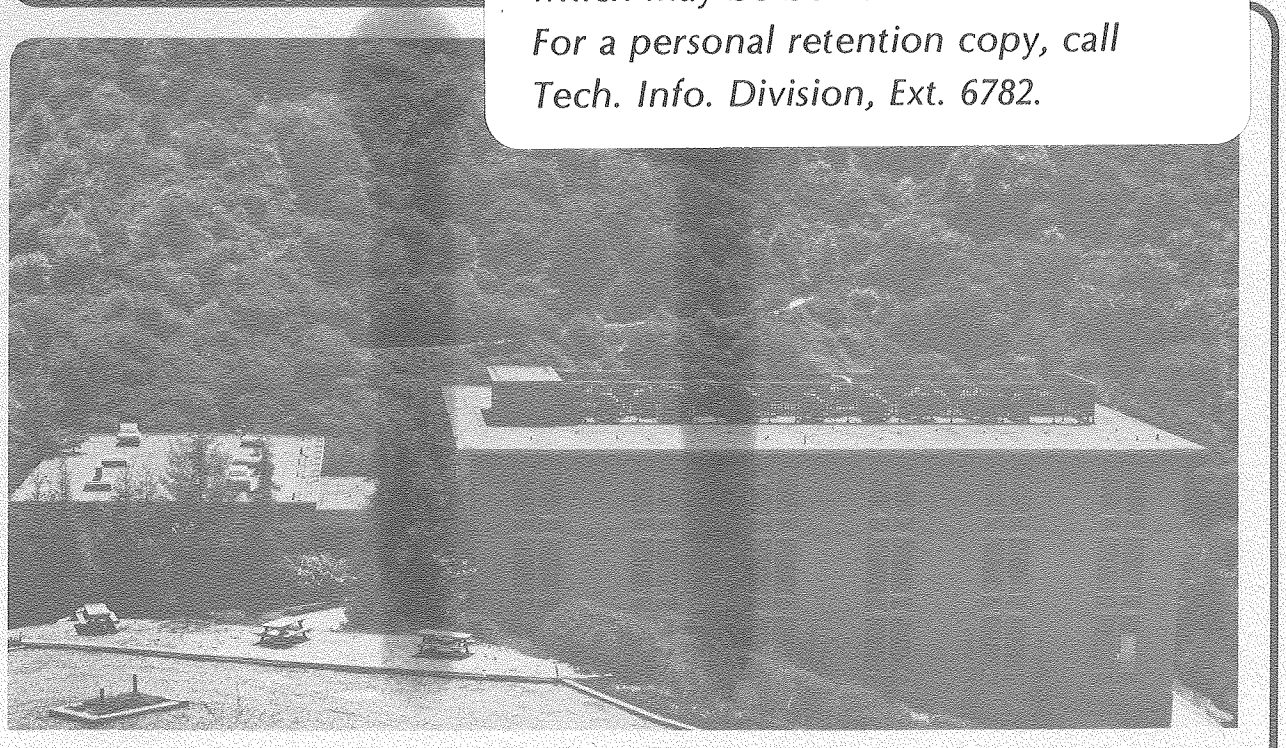

Prepared for the U.S. Department of Energy under Contract DE-AC03-76SF00098

LBL-11777
c.3

DISCLAIMER

This document was prepared as an account of work sponsored by the United States Government. While this document is believed to contain correct information, neither the United States Government nor any agency thereof, nor the Regents of the University of California, nor any of their employees, makes any warranty, express or implied, or assumes any legal responsibility for the accuracy, completeness, or usefulness of any information, apparatus, product, or process disclosed, or represents that its use would not infringe privately owned rights. Reference herein to any specific commercial product, process, or service by its trade name, trademark, manufacturer, or otherwise, does not necessarily constitute or imply its endorsement, recommendation, or favoring by the United States Government or any agency thereof, or the Regents of the University of California. The views and opinions of authors expressed herein do not necessarily state or reflect those of the United States Government or any agency thereof or the Regents of the University of California.

WELDABILITY OF GRAIN-REFINED Fe-12Ni-0.25Ti STEEL FOR CRYOGENIC APPLICATIONS

D. E. Williams and J. W. Morris, Jr.

Lawrence Berkeley Laboratory
University of California
Berkeley, CA 94720

ABSTRACT

The weldability of a research alloy designed for structural use in liquid-helium-temperature cryogenic environments was investigated. Plates of iron-12 weight percent nickel-0.25 weight percent titanium were grain-refined by the four-step, grain-refining thermal treatment developed for this alloy. These plates were then welded with Inconel No. 92 weld wire using the Gas Metal Arc (GMA) welding process with argon-15% helium gas shielding. Both a single pass and a double-sided, 2 pass electron beam (EB) weld were also made but without filler metal addition. Weldments were radiographed and sectioned and the Charpy V-notch specimens removed were tested at liquid-nitrogen and -helium temperatures.

Radiographically acceptable weld deposits were somewhat difficult to achieve. Only 4 out of 7 GMA welds and 2 out of 4 EB welds were acceptable. The problems encountered during EB welding were largely due to alignment and weld metal fluidity. The automated GMA welds encountered problems due to incomplete fusion, the sensitivity of the weld metal to oxidization and the production of inclusions rich in titanium. The minimum Charpy V-notch impact values obtained for the heat-affected zones of a radiographically acceptable GMA weld were 50 and 62 ft-lbs (68 and 84 Joules) at liquid helium (4°K) and liquid nitrogen (-196°C) testing temperatures, respectively. Weld metal toughness for Electron Beam welds were 15 and 23 ft-lbs (20 and 31 Joules)

at these test temperatures. HAZ Charpy impact values were 18 and 24 ft-lbs (24 and 39 Joules), respectively, for the single pass, and 33 and 96 ft-lbs (45 and 130 Joules), respectively, for the two pass welds. Typical Charpy impact values for the base metal are 95 and 120 ft-lbs (129 and 163 Joules) at these two temperatures.

Additional specimens were subjected to simulated HAZ thermal treatments. Testing at liquid helium and nitrogen testing temperatures revealed inconsistencies which are still under investigation.

INTRODUCTION

Requirements for structural materials in the expanding cryogenic technology demand combinations of high strength coupled with high toughness at temperatures to that of liquid helium (4°K). For example, one very preliminary set of criteria for the structural materials for the cases of superconducting magnets for advanced fusion reactors suggests a yield strength in excess of 180 Ksi (1240 MPa) with fracture toughness above about 150 Ksi$\sqrt{in}$ (165 MN/$m^{3/2}$)[1]. The scale of this application will most likely preclude any form of post weld heat treatment, thereby eliminating materials such as precipitation hardening steels from the already short list of potential materials. Since, in all but possibly the nitrogen-strengthened grades (e.g. Nitronics), austenitic stainless steels do not have a sufficiently high yield strength at cryogenic temperatures, ferritic steels are being studied even though these materials are ferromagnetic and undergo a brittle transition. One such steel, which was developed at UCB/LBL[2,3], meets these requirements with less than 13% alloying elements.

Although in the as-normalized state (15 μm grain size: ASTM #9) the fracture toughness of Fe-12Ni-0.25Ti is only 75 Ksi$\sqrt{in}$ (80Mn $m^{-3/2}$) at 6°K, over 239 Ksi$\sqrt{in}$ (260 Mn $m^{-3/2}$) are obtained when the grain size is reduced to approximately 1 μm (ASTM #18) by a thermal cycling procedure developed for this alloy[2]. Since its yield strength at this temperature is 195 Ksi (1345 MPa) this alloy seems to be well suited to the need. However, both the commercial feasibility of the four-step heat treatment and the weldability of the grain-refined alloy must be proven.

Although weldability studies have been performed on Fe-12Ni-0.25Ti and two similar alloys[4], the present investigation was based upon the desire to extend the usefulness of this alloy to larger structures, higher deposition

rates and lower temperatures. Where the Develetian, et al.[4], study demonstrated successfully the weldability of this alloy using autogeneous gas tungsten arc (GTA) welding for thin-wall, liquified natural gas containers, the present investigation sought to determine the effects of using the GMA process in thicker (1/2 inch) sections for liquid helium service.

The approach used in the present investigation sought to determine the extent of the degradation of properties within the heat-affected zone through the use of dissimilar filler metal GMA weldments, autogeneous electron beam (EB) weldments and HAZ simulation specimens. GMA weldments were made using Inconel filler wire and were impact tested at liquid nitrogen and liquid helium testing temperatures. In addition, single and two pass autogeneous EB weldments were similarly evaluated. In both processes, welding was accomplished on fully automatic equipment. To isolate fusion zone effects from HAZ properties, specimens were heat treated to simulate HAZ conditions and similarly impact tested at the two cryogenic temperatures.

MATERIAL PREPARATION, WELDING AND SPECIMEN PREPARATION

Alloys of nominal composition Fe-12Ni-0.25Ti with low carbon were induction melted in an argon atmosphere then cast into 20 pound ingots in a copper chill mold. A typical chemical analysis is shown in Table I. Homogenization was performed under vacuum at 1200°C (2200°F) for 24 hours. The ingots were then upset cross forged at 1100°C (2000°F) into 1/2 inch (13mm) thick by 7-9 inch (180-230mm) wide plates. Each plate was then annealed at 900°C (1650°F) for two hours to remove prior deformation strain and to provide a constant starting point for subsequent grain refinement.

Grain refinement was accomplished through the four step (2B) heat treatment process previously developed for this alloy[2] with the exception that heating rates were generally slower (12-14°C/min vs 15°C/min) and

water, rather than air, quenching was necessary to compensate for the larger specimen mass. Grain refinement through this four step heat treatment is accomplished by repeatedly heating first to a temperature just above the austenite transformation temperature, or A_{c_3}, holding for two hours and quenching and, secondly, heating to a temperature just below the A_{c_3}, holding for two hours and quenching. The evolution of microstructure is shown in Fig. 1. The practical limit to grain refinement of this material with this process (approximately one-half micron average grain size) will usually be reached in a few repetitions for small samples. This process of grain refinement is based on providing the conditions preferential to nucleation while carefully avoiding those which promote growth. During the first part of the cycle, many austenite grains are nucleated but few grow since there is insufficient thermal energy for the necessary diffusion. The resulting martensite laths are subsequently altered by the two-phase decomposition step since the stable austenite nucleating is chemically different from that previously precipitated. It is important to note, however, that it is not possible to avoid conditions favorable to grain growth during welding.

The plates were then cut and the edge preparations machined. Single and double Vee and single and double bevel end preparations were used. In all cases a 1/32 to 1/16 inch (0.8 to 1.6mm) root face and a 1/32 to 3/32 inch (0.8 to 2.4mm) root opening were employed to attempt full penetration on the root pass.

The parameters used during welding were derived from optimizing the weld contour and penetration by running beads-on-plate with varying open circuit voltages, currents, wire stickouts, travel speeds and shielding gas mixtures. Spray transfer, which was necessary to minimize the introduction of defects on the automated equipment, was detected by recording sample oscillographs of simultaneous (chopped) voltage and current wave forms.

The welding parameters, which were determined by these tests and which remained approximately constant throughout the course of the research, were an open circuit voltage of 41-43 volts, a stickout of 3/4 inch (19mm), and a nominal shielding gas mixture of Ar + 15% He, except as noted in Table II. The variable which was manipulated in order to change the heat input to accommodate differences in weld joint configurations was primarily the travel speed which ranged from 10 to 30 inches per minutes (254 to 762mm/min). However, weld numbers 11 and 12 had arc currents between 270 and 310 amperes while all other GMA welds were made between 240 and 280 amperes. Except for the root pass which was ground out in all but weld 11, welding parameters were kept constant to the extent possible between weld passes of the same weld. No pre-heat was used and interpass temperatures were kept below 60°C (140°F) with water-cooled, copper coils to increase cooling rates. Out of six GMA welds, two were rejected when found by radiography to have extensive regions of incomplete fusion.

Electron beam welds were made at 60 kV, 50 ma and 10 inches per minute (254mm/min) under high vacuum. Four welds were made since radiography revealed the first two contained continuous lines of incomplete fusion near midthickness even though they were two pass welds made from opposite sides. Weld 7 was successfully made from one side with the use of a back-up strip, while weld 8 was again a two pass weld although radiographically sound. Again, no preheat was used and interpass temperatures were kept below 100°C (212°F).

Radiography and relevant surface examinations were performed on all welds. When necessary, liquid penetrant examination was performed between weld passes and ultrasonic examination was used to determine the depth of indications observed on radiographs. Using the radiographs to circumvent any weld defects, the welds were sectioned with all but the first and last 3/4 of an inch (19mm) capable of providing specimens.

The specimens removed included Charpy V-notch, bend and optical. Optical metallography specimens, taken from welds made with Inconel weld wire, were polished and either differentially etched chemically or slightly mechanically etched followed by a cathodic vacuum etch[5]. Due to the drastically different etching responses between the weld and the base metal, only cathodic vacuum etching was successful in allowing high magnifications of the fusion zone, Fig. 2. Only high energy boundaries such as prior austenite grains are expected to be etched since the process, which is similar to the etching of gold during sputtering, depends on the ejection of metal atoms by ion bombardment. This technique was not successful on highly polished specimens. Macro sections were also recorded, Fig. 3.

Mechanical testing was performed at both liquid nitrogen (LN) and liquid helium (LHe) temperatures. Standard Charpy V-notch specimens were impacted within 5 seconds of LN immersion in accordance with the ASTM specifications[6]. Impact specimens of 51mm length were broken in insulated plastic boxes at liquid helium temperature in accordance with a procedure described elsewhere[7].

Temperature profiles occurring during welding were established by recording temperatures from different weld passes with a stationary thermocouple located on the plate surface 3/16 inch (5mm) away from the square bevel of a double bevel (k) weld joint preparation. The thermocouple was thus approximately 3/8 inch (2.5mm) away from the root pass and within 1/32 inch (0.8mm) from the final pass. Simulation specimens 1/2 by 1/2 by 2-1/2 inches (15mm x 15mm x 65mm) were then subjected to similar heat treatments although heating rates were slower (by 1/3) and cooling rates were somewhat faster. The simulation study was conducted on a 25 kW induction furnace with a water quenching medium. Temperatures were determined by an optical pyrometer for temperatures above 750°C (1380°F) and a K-type thermocouple

for temperatures below.

RESULTS AND DISCUSSION

Gas Metal Arc Welds. The results of mechanical testing on welds done in this study are shown in Table III. Except in the case of simulation studies, base metal impact test specimens were taken transverse to the major rolling axis and only one specimen was tested per plate since it was used primarily to determine the effectiveness of the grain refining (2B) heat treatment. Owing to limitations in base plate material and, thus, weld length, the majority of mechanical test specimens taken from the Inconel/GMA welds were extracted so as to test heat-affected zone properties rather than those of the weld metal.

The initial welding procedure was based on the expectation that degradation of the grain-refined structure through both grain growth and tempering would be a principal source of the loss of cryogenic toughness. Although the welding of a metal which has been thermally grain refined to an ASTM grain size of 18 or smaller is a new form of welding problem, stringer passes, low interpass temperatures and low heat input were considered desirable. However, these considerations were modified by the necessity to minimize the defect level. The selection of the GMAW process using Inconel filler metal was based on both current industrial practice in similar cryogenic alloys[8] and the ability to separate weld metal effects from base metal characterization. A ferritic filler metal would have been undesirable since its ductile-to-brittle transition temperature (DBTT) would be confused with that of the HAZ, assuming that the weakest part of the weldment lay within the fusion zone. Inconel No. 92 filler metal was also chosen for its constancy in absorbing impact energy down to liquid nitrogen temperature (119.5 ft-lbs (162 Joules) at room temperature compared with 118.0 ft-lbs (160 Joules at -296°C)[9]. A chemical analysis of the Inconel alloy used is

given in Table IV. The non-reactive gases were used for shielding to avoid introducing any interstitial impurities into the weld as these are known to decrease the toughness of ferritic alloys at cryogenic temperatures.

Although defect types such as incomplete fusion are notorious in GMA welding and would be expected to be considerably worse in a fully automated GMA welding situation, the automated system was chosen out of consideration for improving the confidence that each specimen was representative of the weld since many more variables could be controlled and repeated. The most significant of these variables include travel speed, stickout and oscillation. With this apparatus, however, the optimum transfer mode was necessarily spray. To minimize the heat input to the base plate during welding, a high travel speed, often above 25 inches (635mm) per minute, and a stick out of 3/4 inch (19mm) were necessary.

An optimum shielding gas, argon with approximately 15% helium, was determined by running beads-on-plate with widely varying gas ratio mixtures. The Inconel 92 alloy was found to be extremely sensitive to oxidation. At the welding speeds used, unless a four-inch (10cm) long trailing gas nozzle (pure argon) immediately followed the gun nozzle, a wrinkled oxide skin often obscured even the weld ripples. Oxide inclusions were common on fracture surfaces even in weld beads with bright, unoxidized surfaces. Brittle inclusions or the remains of inclusions, such as in Fig. 4, which shows an inclusion from the fracture surface of a HAZ specimen from weld 3, always registered high in titanium in EDAX analysis, usually in proportion to their volume, but were never sufficiently wide and thick to obtain a background-free count. As thin and broken-up as the remains of the inclusion in Fig. 4 obviously are, an EDAX computer estimate of the weight percent composition (assuming Fe+Ni+Cr+Mn+Ti = 99%) determined titanium at above 83%. Since the beryllium window of the EDAX counter did not allow detection of elements

lighter than fluorine, any titanium oxide, nitride and carbide, etc., would then register high titanium percentages. Fracture surfaces of Inconel weld metal specimens sometimes revealed large areas of titanium-rich surfaces such as the 150 by 50 μm film evidenced in Figs. 5 and 6.

The titanium-rich inclusions were by no means restricted to the Inconel 92 weld deposit but were visible on virtually all base plate fracture surfaces as the small, numerous particles at the base of ductile "cones" (Fig. 7). Although the fracture surfaces of the simulation study specimens were very similar to those of the as-grain-refined (2B) base metal, very little ductility was evident in the electron beam weldments, especially in fracture surfaces representing the weld metal.

In spite of the problems in obtaining weld deposits with acceptable defect levels, the impact toughness of the GMA-welded materials was usually good. Most HAZ toughness values were greater than 50 ft-lbs (68 Joules) in LHe and 60 ft-lbs (81 Joules) in LN for specimens near the fusion zone, which was generally the weakest region of the weldment. The only exceptions to these minima were for specimens with defects observable in non-destructive examinations.

Since the fusion zone was the region of minimum toughness in the weldment in all Inconel/GMA welds, except those deposited in the 'jet-rotation' transfer regime (welds 11 and 12) where HAZ values were unchanged while weld metal properties deteriorated, other tests had to be used to further characterize the weakening mechanism. This mechanism could be caused by chemical interactions with filler metal, the large effective grain size of the partially melted region of the base metal in the fusion zone, or some effect of the heat treatment encountered during welding. To distinguish these required two additional experiments with similar heat treatments given to the metal:

one without added elements in the vicinity of the fusion zone was represented by the autogeneous EB welds and one without a fusion (partially melted) zone was represented by the HAZ simulation studies.

ELECTRON BEAM WELDS

Single and double pass, full penetration electron beam (EB) welds were made in grain-refined (2B) Fe-12Ni-0.25Ti plates. Square bevels without preheat were used to fuse the two plates without the addition of filler metal or flux or the use of oscillation. The fluidity of the weld metal, presumably attributable at least to some extent to the lack of delta ferrite formation in this steel, precluded full penetration, single pass welds being made without a backing strip. Two pass welds were made from opposite sides and factors such as the lack of critical alignment left long areas of incomplete penetration in two of the three two pass welds. The fourth EB weld (No. 7) incorporated a back-up strip to allow a single pass weld to be made without the excessive loss of weld metal.

Although impact toughness was low for EB weldments, low values were expected based on the extremely coarse solidification structure of the weld metal. Optical cross sections of the weld deposit revealed a cellular structure with cell diameters ranging from 5-10 microns while weld metal fracture surfaces were deeply ribbed with virtually through-thickness ridges (Fig. 8) corresponding to the large cell lengths as seen in Fig. 3. The impact toughness of the HAZ, however, rose from that of the weld metal, 14 ft-lbs (19 Joules) in the single pass weld to 33 ft-lbs (45 Joules) in the HAZ of the two pass weldment where it was further removed from the coarse structure of the fusion zone of the final pass and grain refined by it. A comparison of these fracture surfaces broken at -196°C (LN) is given in Fig. 9.

HAZ SIMULATION

The HAZ simulation studies were initiated to attempt to isolate the source of the degradation of properties observed at least to some extent in the HAZ of all welds tested. Using available induction heating equipment, the 1/2 inch (13mm) square specimens were suspended within the r-f coils and released into water when the required temperature had been reached. Heating rates of 50°C/sec to 1350°C and 1050°C (120°F/sec to 2460°F and 1920°F) were achieved in this manner although heating rates of 135°C/sec to 1050°C (275°F/sec to 1920°F) were recorded during welding. The total time above the transformation temperature was, however, approximately the same for both the actual and the simulated heat-affected specimen.

The results of mechanical and Mössbauer tests on these simulated specimens are given in Table V.

HAZ-simulated studies provided a surprising result: specimens subjected to this fast heating rate/immediate fast quench treatment showed enhanced impact toughness. A specimen heated to 620°C (1150°F) (thermocouple pyrometry), 60°C (110°F) below the austenite phase transformation temperature absorbed 123 ft-lbs (167 Joules) which was 15 ft-lbs (20 Joules) above the base metal while all of those heated above 750°C had values greater than 160 ft-lbs (217 Joules), regardless of whether the heat treatment included single or multiple heatings. Multiple heatings included permutations of 1350°C, 1050°C, and 750°C (2460°F, 1920°F and 1380°F). Retained austenite was measured by Mössbauer spectroscopy in three samples and was never significant past the error inherent in the technique (0.5% ± 0.5%). This was also not expected since, although similar increases in impact toughness were found in tempering studies with this alloy[10], the optimum conditions, at 525°C (980°F) for eight hours, were attributed, at least partially, to an introduction

of two volume percent retained austenite.

Simulation studies were subsequently[11] carried out on the same alloy with similar prior conditions in the same apparatus but with oil quenching to simulate slower HAZ cooling rates such as would be expected in preheated or thinner plates or in higher heat input welding processes. This preliminary work has shown a peak in the Charpy V-notch energy absorbed when specimens were reheated to a maximum temperature of about 700°C (1290°F) with values falling to less than 20 ft-lbs (27 Joules) for reheat temperatures of 1300°C (2370°F). The cooling rate actually measured during welding lay between the two simulation rates as it took seven seconds for the weldment to cool from 1000°C to 500°C (1830°F to 930°F), two seconds for the water-quenched specimen and 17 seconds for the oil-quenched one. Although faster cooling rates than those recorded during welding may be expected in heavy wall fabrication made without preheat, the slower cooling rates of the higher deposition processes are desirable. It is suspected that the critical cooling rate for this alloy may lie within this range and a CCT diagram is presently being developed.

CONCLUSIONS

The research undertaken to determine the weldability of grain-refined (2B) Fe-12Ni-0.25Ti steel plate in the as-welded state for cryogenic, structural applications revealed that reasonable impact toughness could be retained in spite of the grain coarsening and tempering effects of GMA fusion welding.

Gas metal arc welding, using Inconel No. 92 welding wire with Ar-15% helium shielding gas, produced welds with 50/62 ft-lbs (68 and 84 Joules) minimum HAZ toughness at liquid helium and nitrogen temperatures, respectively, for welds which would be radiographically acceptable under AWS D1.1 or ASME Section VIII, Division 1, Article UW-51 codes. A weld which contained a

clearly excessive amount of porosity (weld 11) yielded a minimum HAZ specimen of 32 ft-lbs (43 Joules) in the HAZ, a value which is still acceptable in many applications.

Inconel 92 filler metal, however, contains an excessive amount of titanium and is too sensitive to atmospheric contamination to be an optimum filler metal.

Electron Beam Welds without any oscillation or filler metal failed at low impact energies, less than 15 ft-lbs (20 Joules), both in the weld metal and HAZ when the as-solidified structure was within the fracture path. When the as-solidified structure was tempered and refined by a second pass, the HAZ specimen tested in liquid helium absorbed 33 ft-lbs (45 Joules).

Samples of the plate material were subjected to thermal treatments bracketing those measured in the HAZ of a GMA weld. Although specimens with faster cooling rates than measured in the weld showed uniform improvement of impact properties over the base metal, increasing to over 160 ft-lbs (215 Joules) for specimens whose simulation temperature traversed the austenite phase transformation temperature (A_{c_3}), other work has shown deterioration of impact toughness when slower cooling rates were used. Continuous cooling phase transformation data is presently being obtained to better understand this phenomenon.

ACKNOWLEDGMENTS

This work was supported by the Director, Office of Energy Research, Office of Development and Technology, Magnetic Systems Division of the U.S. Department of Energy under Contract No. DE-AC03-76SF00098.

REFERENCES

1. Dalder, E.: Private communication.

2. Jin, S., Morris, J. W., Jr. and Zackay, V. F.: Grain Refinement through Thermal Cycling in an Fe-Ni-Ti cryogenic Alloy, Met Trans A, vol. 6A, p. 141, 1975.

3. Jin, S., Hwang, S. K. and Morris, J. W., Jr.: Comparative Fracture Toughness of an Ultrafine Grained Fe-Ni Alloy at Liquid Helium Temperature, Met Trans A, August, 1975.

4. Devletian, J. H., Stephens, J. R. and Witzke, W. R.: Weldability of High Toughness Fe-12% Ni Alloys Containing Ti, Al or Nb, Welding Journal, April, 1977.

5. Padden, T. R. and Cain, F. M., Jr.: Cathodic Vacuum Etching, Metal Progress, p. 108, July 1, 1954.

6. ASTM E 23 and ASTM A 370.

7. Jin, S., Horwood, W. A., Morris, J. W., Jr. and Zackay, V. F.: A Simple Method for Charpy Impact Testing below 6°K, Advances Cryog Eng, vol 19, p. 373, 1974.

8. Pense, A. W. and Stout, R. D.: Fracture Toughness and Related Characteristics of the Cryogenic Nickel Steels, WRC Bull, 205, May, 1975.

9. Shoemaker, L. E., Huntington Alloys, Technical Service and Specifications Dept.: Private communication.

10. Hwang, S. K., Jin, S. and Morris, J. W., Jr.: A Study of Retained Austenite in a Fine Grained Fe-12Ni-0.25Ti Alloy, Met Trans A, vol 6A, p. 2015, 1975.

11. Kim, H. J.: private communication.

TABLE I. Typical Composition of Fe-12Ni-0.25Ti Ingots.

Ni	Ti	C	N	S	P	Mn	O	Fe
11.5	0.23	0.009	0.003	<0.005	<0.005	<0.005	0.02	Balance

TABLE II. Welding Parameters.

Weld	Type	Bevel	No. of Passes (Front & Rev. Sides)	Heat Input (KJ/mm)	Shielding
2	GMA	2-V	4 + 4	0.32	Ar-20%He
3	GMA	K	5 + 4	0.66	Ar-40%He
11	GMA	sgl.bvl.	5	0.98	Ar-17%He
12	GMA	sgl.bvl.	6 + 1	0.95	Ar-14%He
7	EB	sqr.	1	0.71	vacuum
8	EB	sqr.	1 + 1	0.71	vacuum

1 inch = 25.4 mm.

TABLE III. Weld Results.

Weld Number	Charpy V-notch Impact Energies (Ft-lbs) Given as: Average value (No. of specimens) Minimum value				
	Weld Metal		HAZ		Base Metal
	L.N	L.He	L.N	L.He	L.N
2	88(2) 87		88(4) 83	96(1)	96(1)
3	72(1)		76(3) 62		106(1)
11	53(1)	88(1)	75(4) 60	80(1)	100(1)
12	66(2) 65		43(4) 32	50(2) 50	106
7	23(1)	15(1)	29(4) 26	18(2) 13	106
8	23(2) 21	13(1)	81(3) 50	33(1)	100

1 Joule = 1.356 ft-lbs

TABLE IV. Chemical Analysis of Inconel No. 92 Weld wire (Heat No. HT1961MD).

C	Mn	Fe	S	Si	Cu	Ni	Cr	Ti	Others
0.03	2.27	8.28	0.008	0.05	0.11	69.99	16.04	3.22	<0.50

TABLE V. Simulation Results.

Specimen	Heat Treatment	Retained Austenite (Mössbauer)	Charpy V-notch Im. Energies (Ft-lbs) L.N	L.He
14,15	2B	0-1/2% ±1/2%	108	
1,2,3	+1050°C WQ+1350°C WQ+750°C WQ		161	132
4,6,7	+1350°C WQ 1050°C WQ+750°C WQ		163	135
8	+1350°C WQ+750°C WQ		167	
9	+1350°C WQ	1/2% ±1/2%	163	
10	+750°C WQ	0-12% ±1/2%	166	
11	+700°C WQ		131	
12	+650°C WQ		148	
13	+620°C WQ		123	

°C = 5/9 (°F-32) 1 Joule = 1.356 Ft-lbs

FIGURE CAPTIONS

1. Microstructural evolution of 2B heat treatment.
2. Root area of double vee weld #2: Inconel/GMAW.
3. Macrosections of welds #2(GMA), #7 and #8 (EB).
4. Heat-affected zone specimen (weld #3) fracture surface: Inconel/GMAW.
5. Weld metal specimen (weld #3) fracture surface: Inconel/GMAW.
6. Detail of Fig. 5.
7. Base metal region (weld #3) fracture surface.
8. Weld metal specimen (weld #7) fracture surface: EBW.
9. Fracture surface comparison of electron beam welds (LN).

ELECTRON BEAM WELDS

WELD METAL

C_v = 23 ft-lb

FUSION ZONE - HAZ

C_v = 29 ft-lb

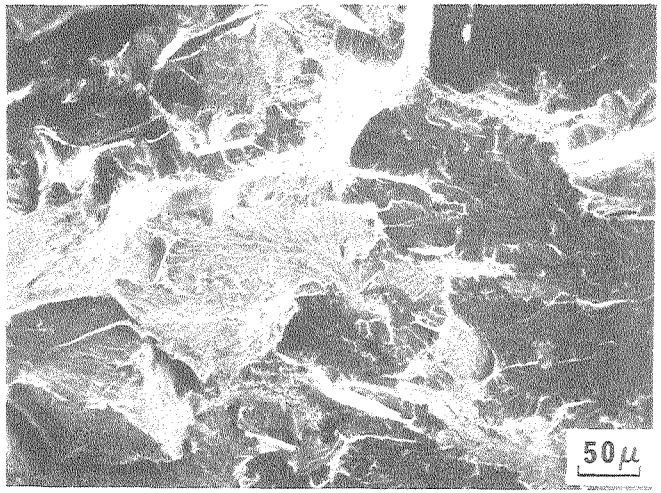

1 PASS

-196°C

C_v = 23 ft-lb

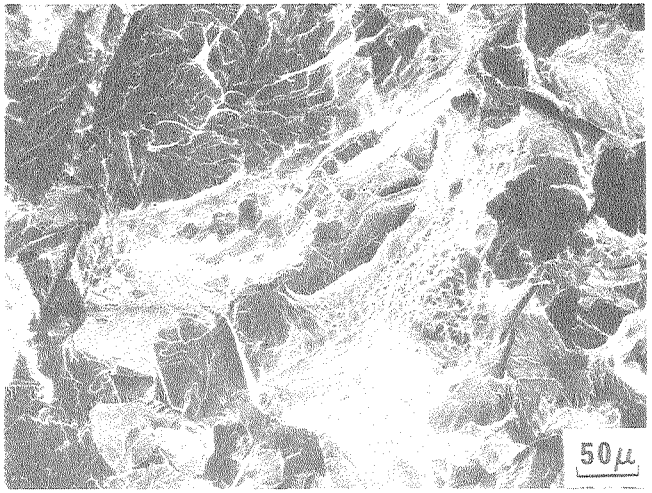

2 PASS

C_v = 65 ft-lb

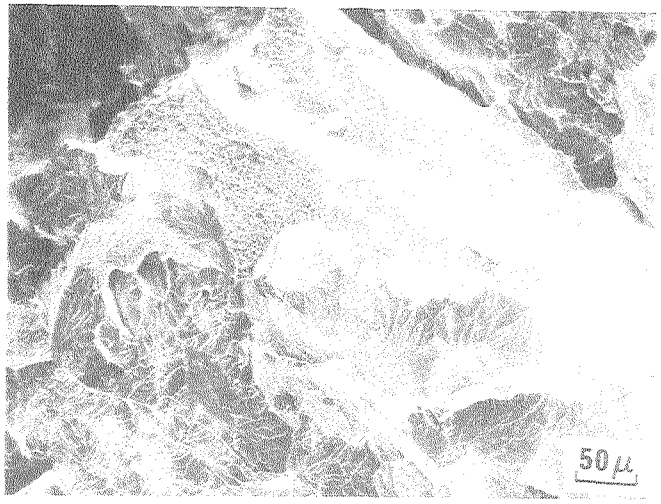

Figure 1

XBB 739-5684

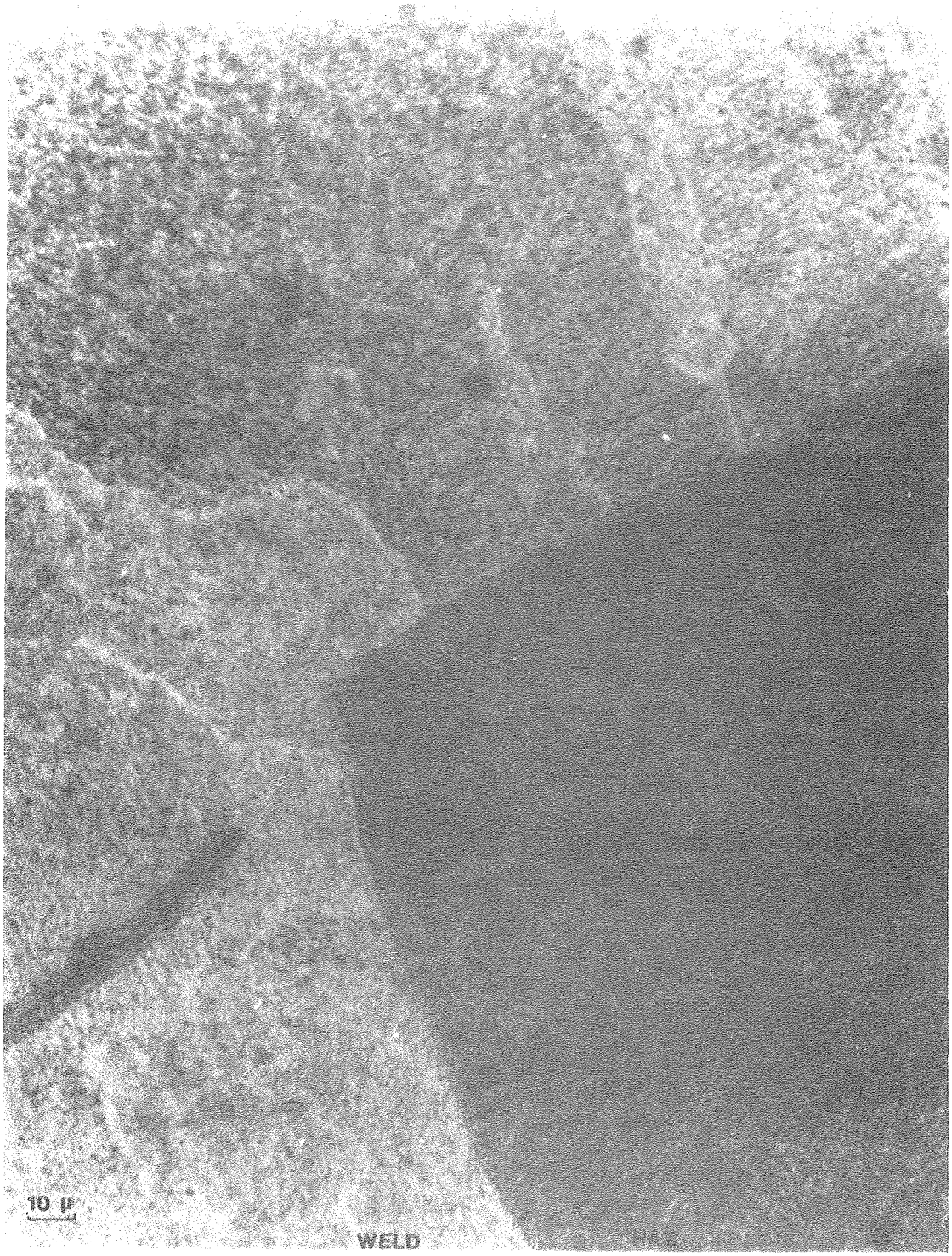

Figure 2

XBB 799-12813

WELDED SPECIMENS

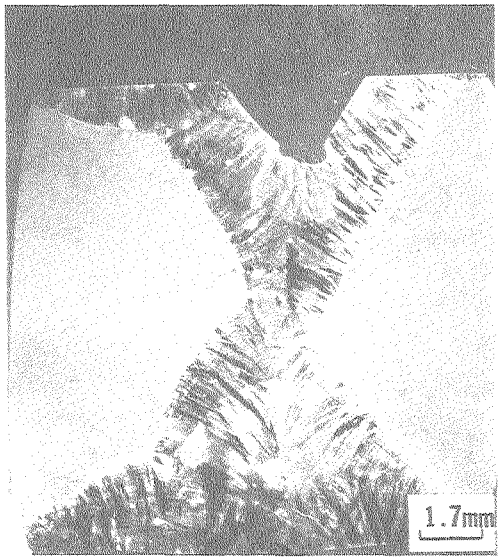

GMA WELD Dbl-V

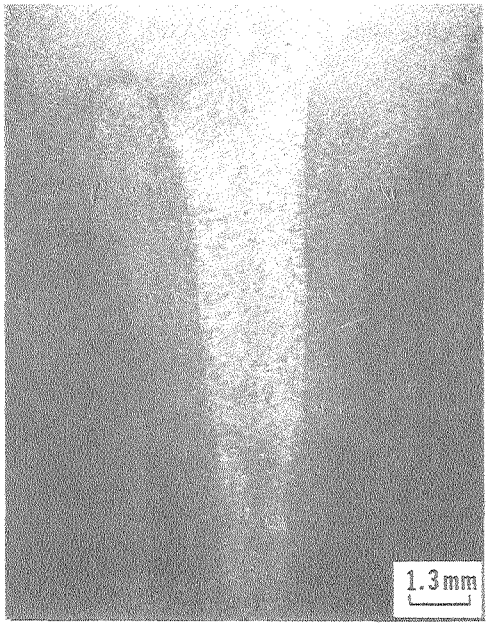

EB WELD 1 Pass

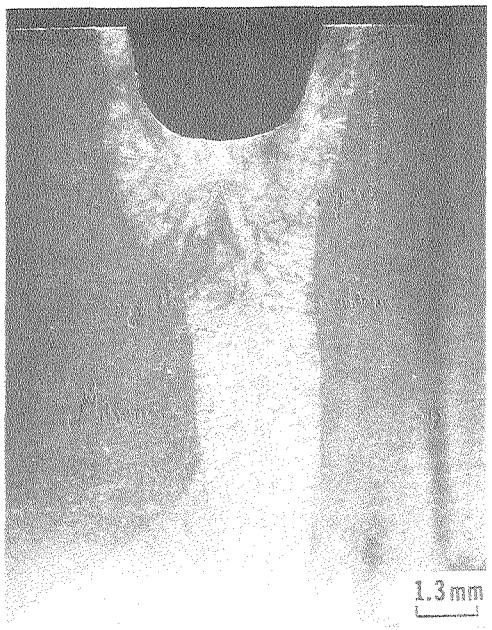

EB WELD 2 Pass

Figure 3

XBB 799-12640

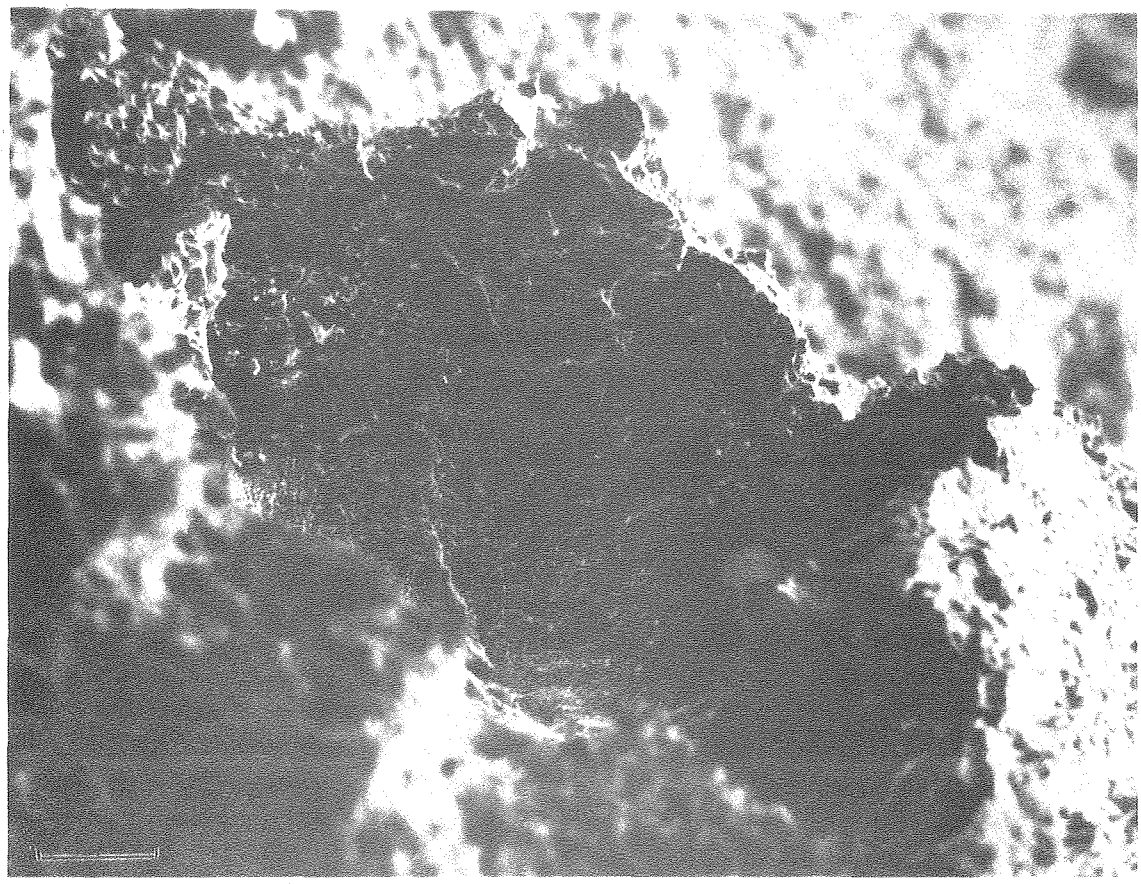

Figure 4

XBB 799-12815

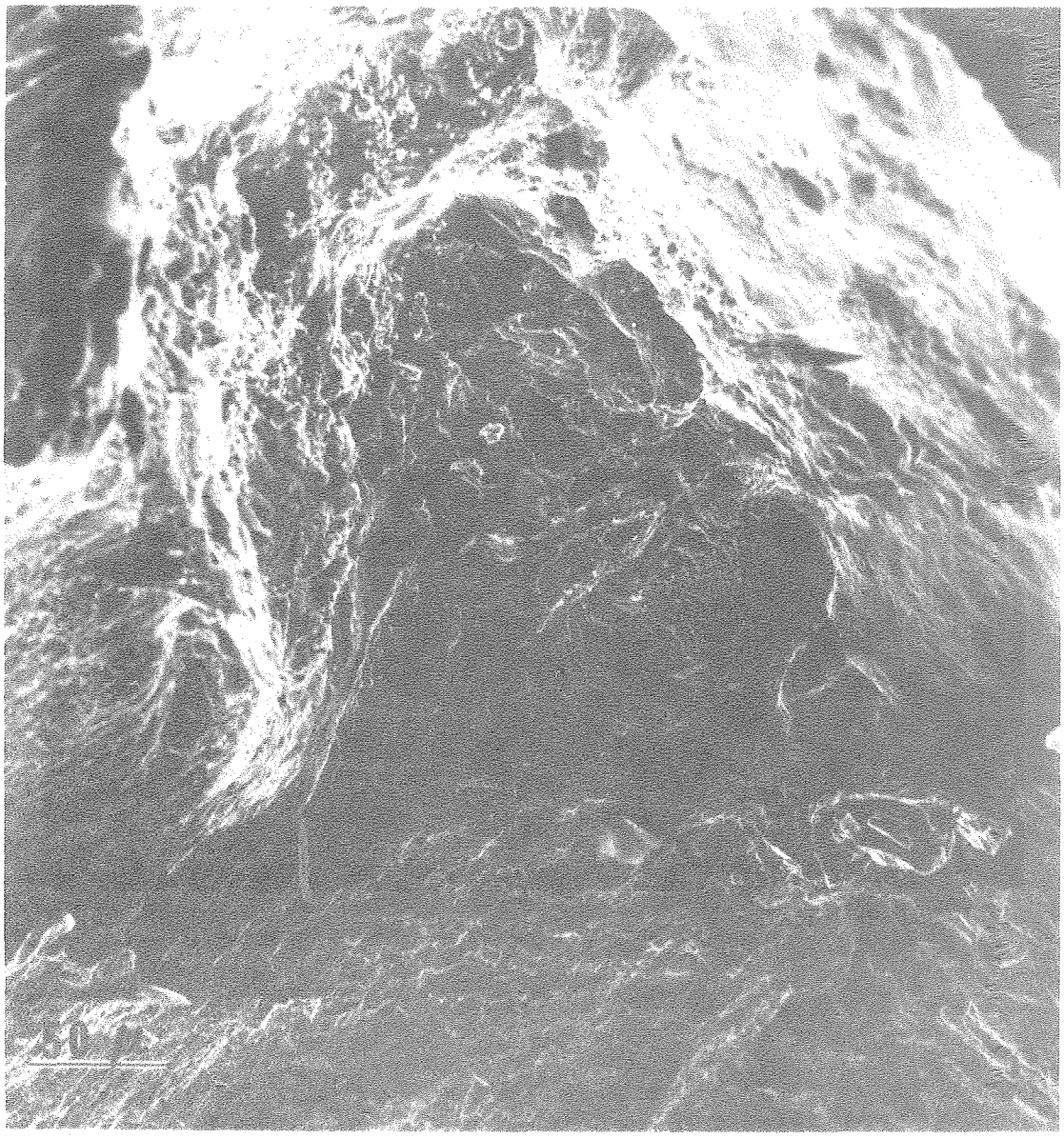

Figure 5

XBB 799-12820

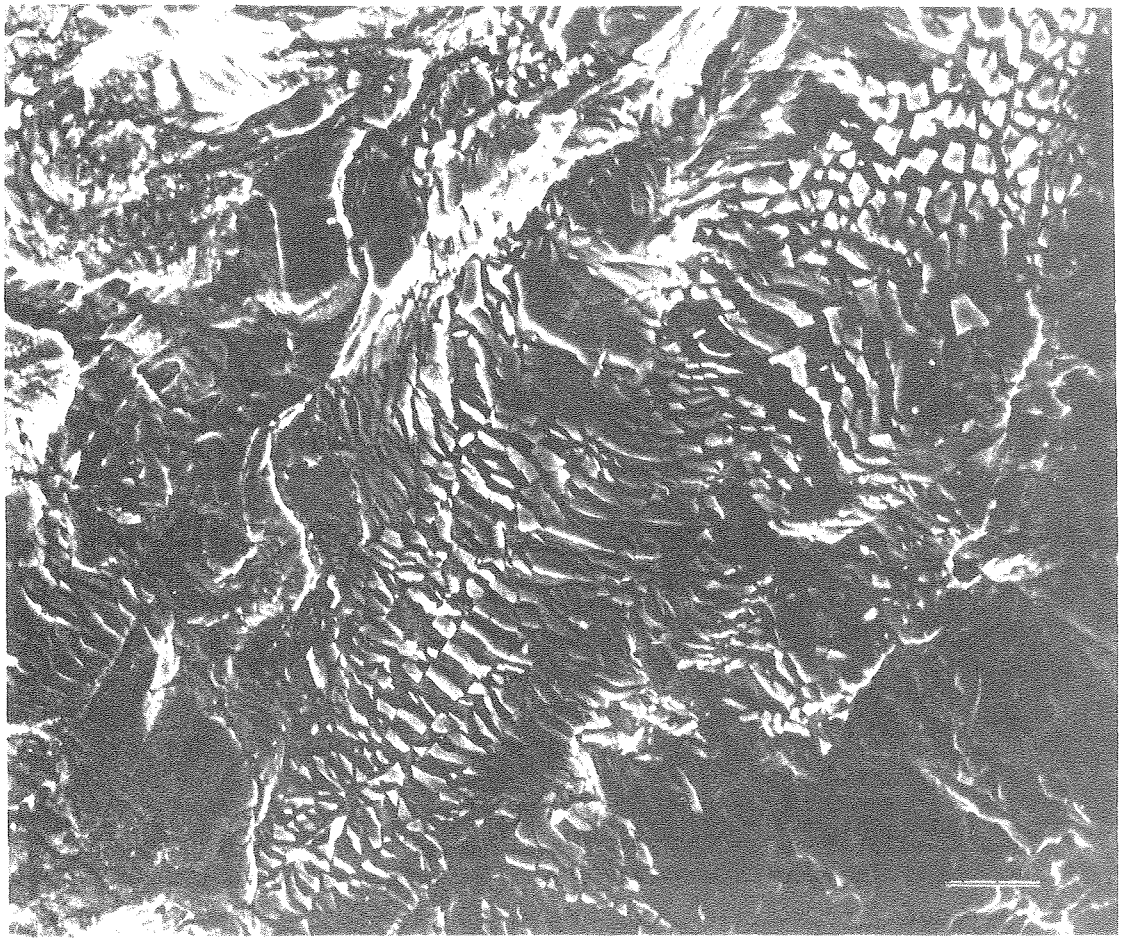

Figure 6

XBB 799-12816

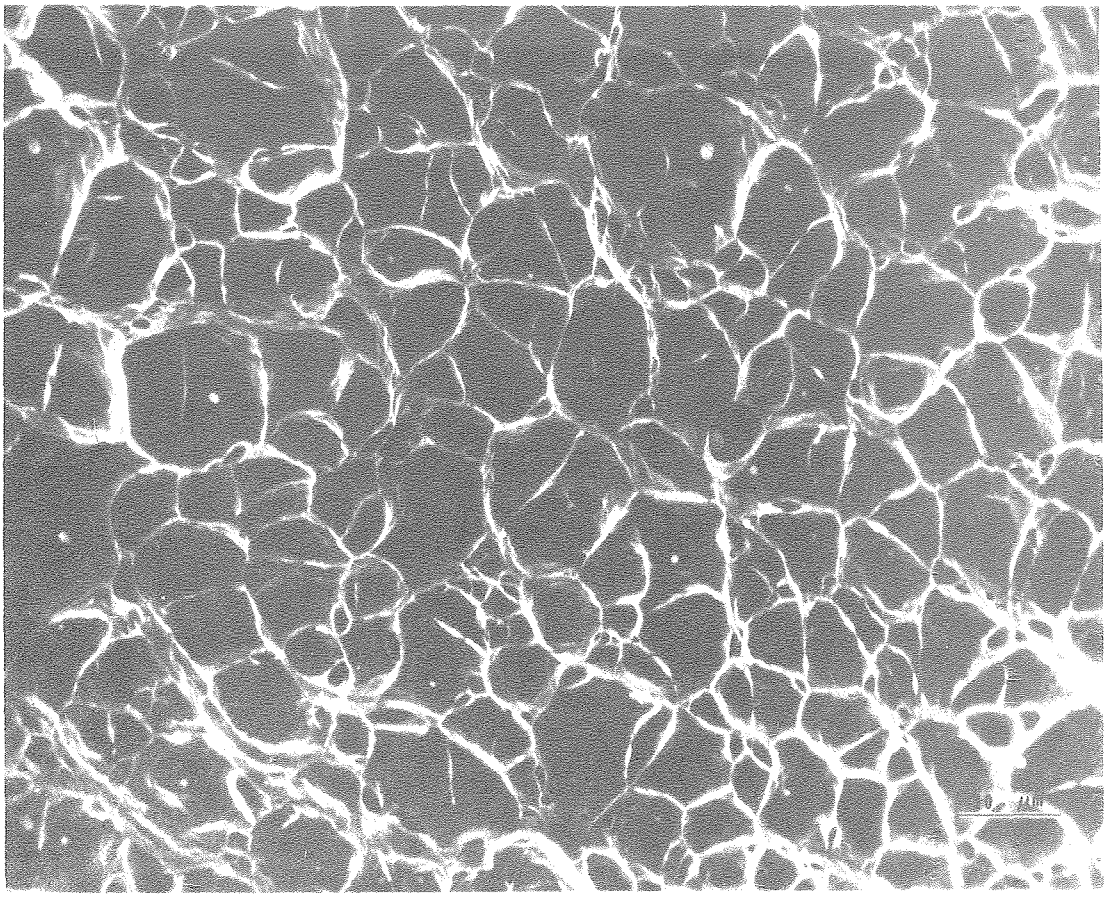

Figure 7

XBB 799-12817

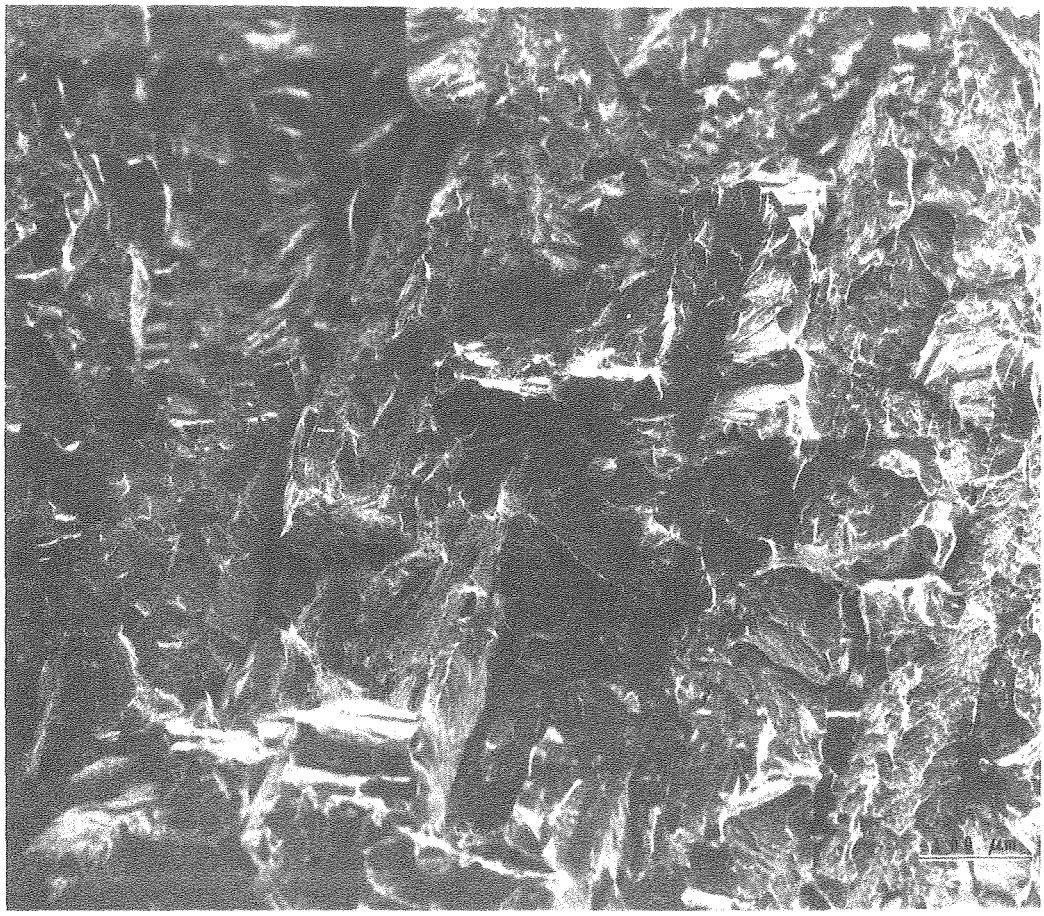

Figure 8 XBB 799-12819

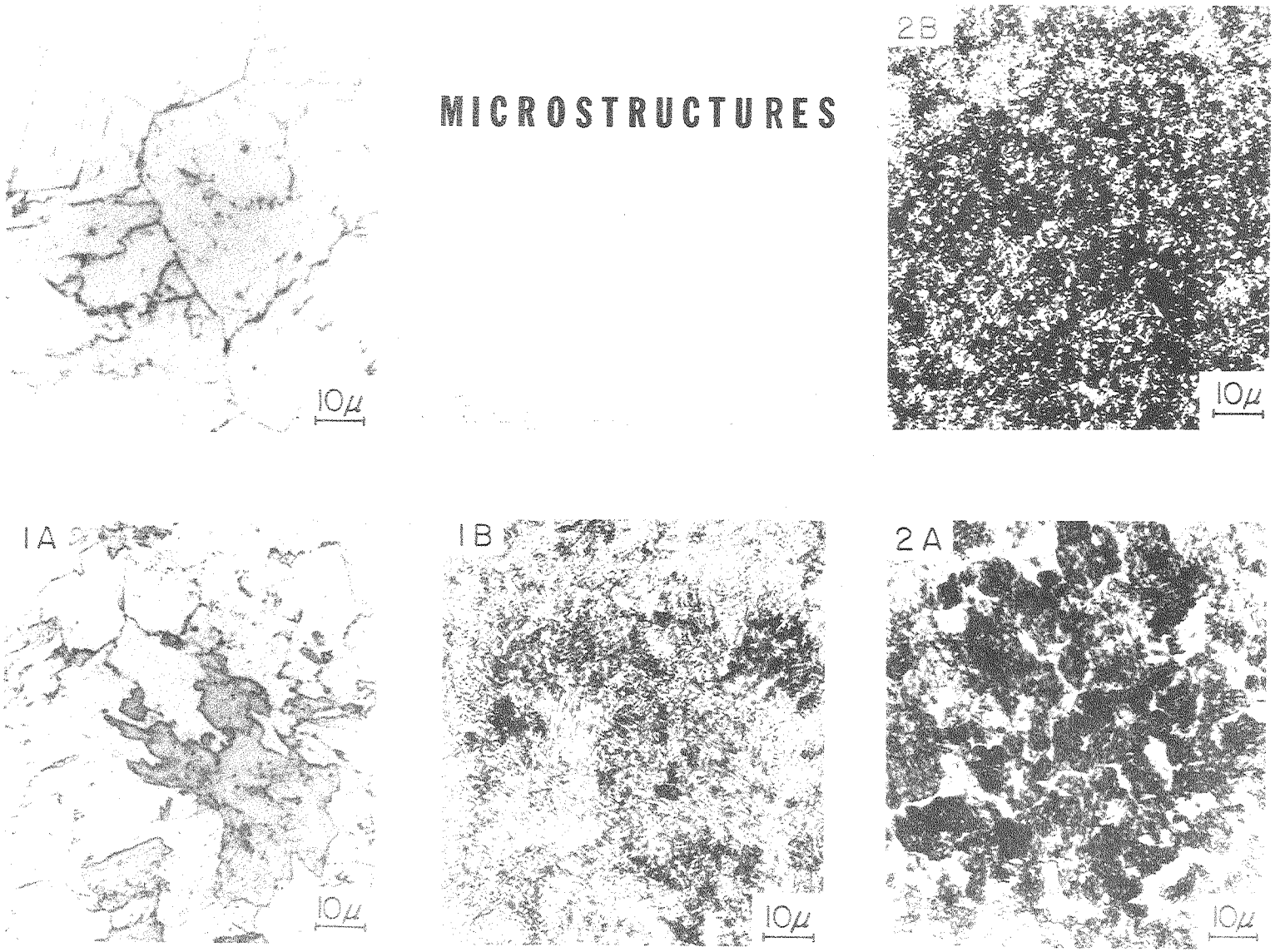

Figure 9

XBB 799-12639